Supporting Information: Acceleration of Butane Vapor Nucleation by Carbon Dioxide Gas

Arnab Choudhury[a,‡], Felix Graber[a,‡], Stefan Feusi[a], Jan Krohn[a], Jai Khatri[a], Fernando Torres Hernandez[a], Chenxi Li[b], Ruth Signorell[a,*]

[a]ETH Zürich, Department of Chemistry and Applied Biosciences, Vladimir-Prelog-Weg 1-5/10, 8093 Zürich, Switzerland
[b]School of Environmental Science and Engineering, Shanghai Jiao Tong University, Shanghai 200240, China
[‡]These authors contributed equally.
[*]Corresponding author: rsignorell@ethz.ch

S1 Water unary and water-CO_2 binary vapor nucleation

Figure S1 shows the data for the unary nucleation of water (panel A) and for binary nucleation of the water-CO_2 mixture (panel B) as published in Ref.[1]. Here we have re-analyzed the data with the inclusion of ξ in Eqs. 6 and 9. It should be noted that the rate constants $k_{1,1}$ for unary water nucleation and β for water-CO_2 binary nucleation increased by a factor of two compared to that reported in Ref.[1], owing to the inclusion of ξ in the present model.

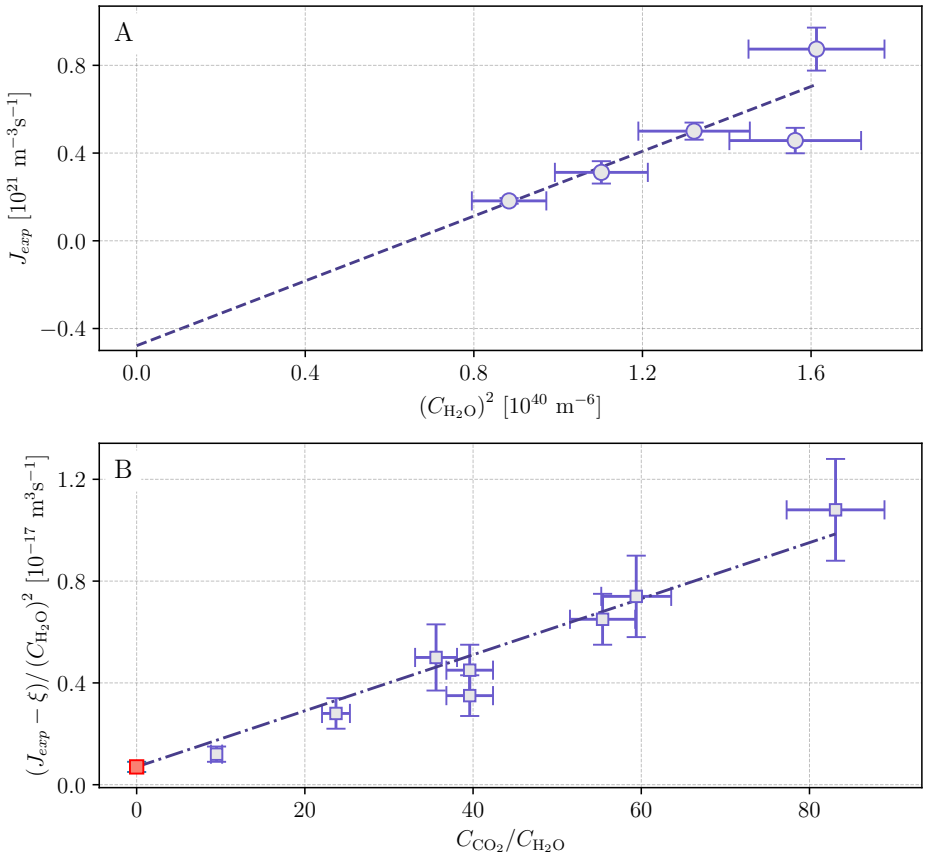

Figure S1: **(A)** Unary water nucleation. Circles: Experimental data points J_{exp} as a function of $(C_{H_2O})^2$. Dashed line: Linear fit using Eq. 6 and $J_{exp} = J_{un}$. **(B)** Water-CO_2 binary nucleation. The red marker denotes $k_{1,1}$. The dashed-dotted line denotes the linear fit according to Equation 10 and $J_{exp} = J_{bi}$. The β value obtained in the fit is given in Table 1.

S2 Simulated behavior of J

We simulated the behavior of J assuming different experimental artifacts, such as cluster loss during ionization and limitations due to detection. To begin, Eq. 6 was used to generate J_{model} with $k_{1,1}$ ($\xi = 0$) for different values of C_{Bu}, shown as the solid black lines in Fig. S2. From these values, the total number concentration was obtained by integrating J_{model} over time,

$$C_{tot}(t_i) = \int_{t_0}^{t_i} J_{model}\, dt \quad (i = 1, 2, 3, \ldots). \tag{S1}$$

A cluster mass distribution was then generated that resembled the experimental data, ensuring that the total cluster concentration matched $C_{tot}(t_i)$.

This simulated distribution was subsequently screened according to the relevant conditions, such as cluster loss or being below the detection limit. The resulting concentrations yielded the simulated nucleation rates, J_{sim}, which are shown as open circles in Fig. S2. Linear fits through the J_{sim} values, indicated by the dashed-dotted lines, demonstrate that in both cases the fits pass through the origin.

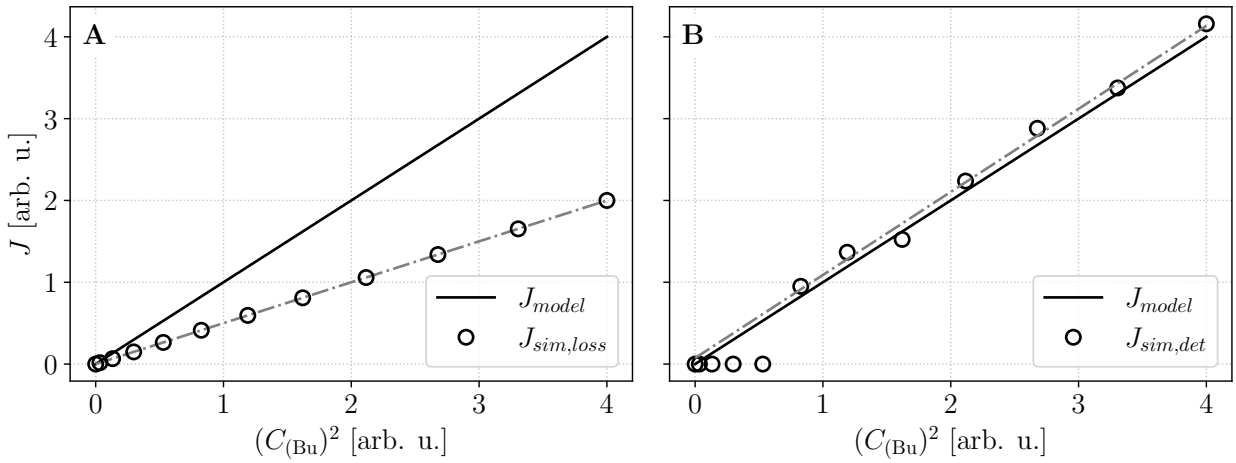

Figure S2: Simulated behavior of unary nucleation rates with monomer number concentration squared for **(A)** loss of cluster during ionization and **(B)** due to detection limit of the instrument. Black solid lines: Generated J_{model} values according to Eq. 6 with $\xi = 0$. Black circles: Simulated J_{sim} data points. Gray dashed-dotted lines: linear fit through the simulated data points using Eq. 6.

S3 Baseline rise due to mixed clusters

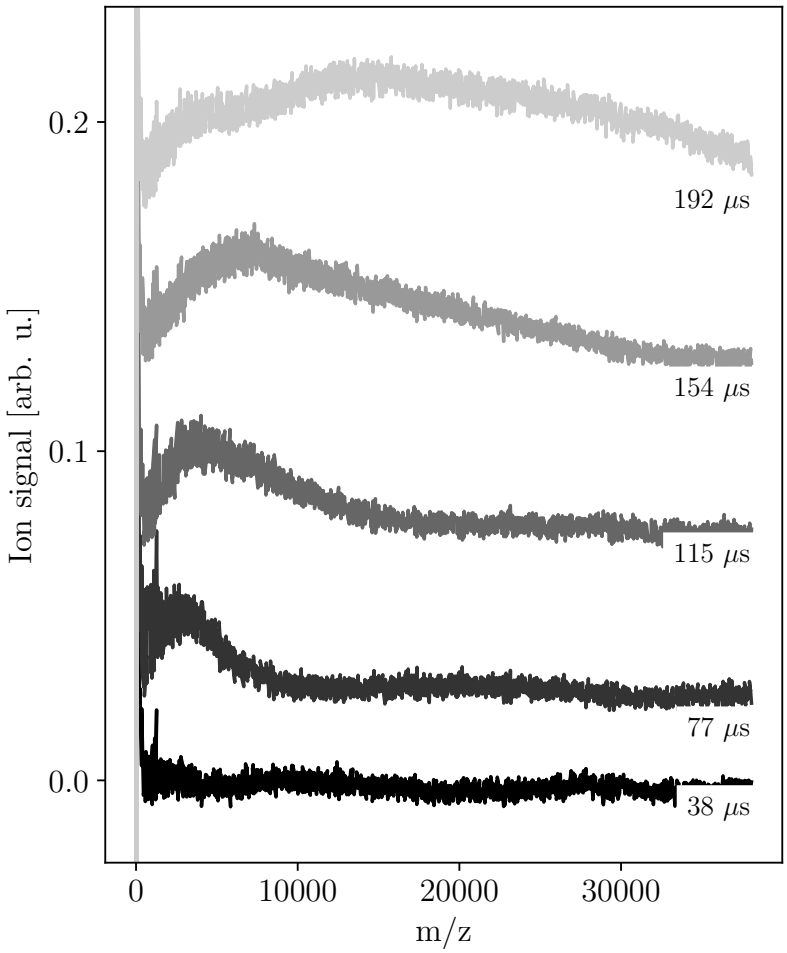

Figure S3: Mass spectra for a mixture of 0.21% Bu (1.2×10^{20} m^{-3}) and 12.7% CO2 (7×10^{21} m^{-3}), same conditions as Fig. 6 (middle row), without baseline correction. The baseline drifts/rises at larger cluster sizes (masses) are an indication for the formation of mixed clusters. For shorter times, the abundance of mixed clusters with lower masses (Fig. 6) is very low and often below the detection limit. At longer times, the mixed clusters of higher masses are visible in the spectra as baseline drifts/rises ("unresolved bums") as the individual mass peaks can no longer be resolved in the spectra. At shorter nucleation times (black curve) this bump is still small, but the center of this bump moves towards higher masses and becomes broader at longer nucleation times (gray scale).

S4 Summary of butane unary and butane CO_2 binary results

Table S1: Overview table for unary butane nucleation measurements. The columns contain: The butane concentration, the nitrogen concentration, the argon concentration, the experimental nucleation rate, the error of the experimental nucleation rate, the temperature of the expansion, the pressure in the expansion as well as the supersaturation of the monomer.

C_{Bu} [10^{20} m^{-3}]	C_{N_2} [10^{21} m^{-3}]	C_{Ar} [10^{22} m^{-3}]	J_{exp} [10^{22} $m^{-3}s^{-1}$]	Error [10^{22} $m^{-3}s^{-1}$]	Temp. [K]	Pressure [Pa]	Sup. sat. [ln(S)]
1.08	7.16	4.95	0.45	0.04	50.8	40	45
1.08	7.13	4.94	0.21	0.03	51	40	44
1.1	7.27	5.03	0.08	0.02	50	40	46
1.19	7.12	4.94	0.31	0.05	51	40	44
1.26	7.16	4.97	0.41	0.03	50.7	40	45
1.27	7.22	5.01	0.54	0.06	50.2	40	46
1.32	7.16	4.97	0.81	0.08	50.6	40	45
1.37	7.11	4.94	0.95	0.12	50.9	40	45
1.43	7.15	4.97	1.1	0.16	50.6	40	45
1.73	7.17	5.01	2.87	0.26	50.3	40	46
2.02	7.16	5.02	5.23	0.36	50.1	40	46
2.3	7.09	4.99	6.14	0.57	50.4	40	46

Table S2: Overview table for binary Butane-CO_2 nucleation measurements. The columns contain the butane concentration, the CO_2 concentration, the ratio of CO_2 to butane, the nitrogen concentration, the argon concentration, the experimental nucleation rate, the error of the experimental nucleation rate, the experimental nucleation rate normalized according to equation 10, error of this normalization, flow temperature, pressure in the flow and monomer super saturation. The super saturation was calculated using the Wagner Equation and coefficients from Ref[2] for the equilibrium vapor pressure.

C_{Bu} [10^{20} m^{-3}]	C_{CO_2} [10^{20} m^{-3}]	C_{CO_2}/C_{Bu}	C_{N_2} [10^{21} m^{-3}]	C_{Ar} [10^{22} m^{-3}]	J_{exp} [10^{21} m^{-3}s^{-1}]	Error [10^{21} [m^{-3}s^{-1}]	$(J_{exp}-\xi)/(C_{Bu})^2$ [10^{-18} m^{3}s^{-1}]	Error [10^{-18} m^{3}s^{-1}]	Temp. [K]	Press. [Pa]	Sup. sat. [ln(S)]
1.08	5.4	5	6.61	4.95	3.99	0.26	1.97	0.33	50.9	40	44
1.1	10.96	10	6.16	5.02	2.69	0.52	1.81	0.31	50.1	40	46
1.09	10.88	10	6.12	4.99	2.3	0.26	1.8	0.31	50.4	40	45
1.09	14.46	13.2	5.8	5.01	5.39	0.95	2.04	0.33	50.2	40	45
1.08	21.68	20.1	4.99	4.96	3.53	1.1	1.93	0.33	50.8	40	45
1.09	27.21	25.1	4.47	4.98	3.2	0.25	1.88	0.32	50.6	40	45
1.08	27.04	25.1	4.44	4.95	4.42	1.53	2.01	0.35	50.9	40	44
1.09	32.68	30	3.95	4.99	5.33	1.2	2.05	0.34	50.4	40	45
1.09	38.12	35	3.4	4.99	10.49	1.25	2.49	0.37	50.4	40	45
1.08	37.75	35	3.37	4.94	4.38	1.26	2.01	0.34	50.9	40	44
1.08	43.52	40.1	2.83	4.97	7.3	1.55	2.23	0.36	50.6	40	45
1.07	48.34	45	2.28	4.92	8.93	1.03	2.42	0.37	51.1	40	44
1.07	53.78	50.2	1.73	4.91	6.65	0.64	2.23	0.35	51.2	40	44

Table S3: Mixed clusters and their corresponding masses [amu] observed in Figure 6 **D**.

	$(Bu)_1$	$(Bu)_2$	$(Bu)_3$	$(Bu)_4$	$(Bu)_5$	$(Bu)_6$	$(Bu)_7$	$(Bu)_8$	$(Bu)_9$
$(CO_2)_1$	-	160.25	218.37	276.49	-	392.73	450.85	508.97	567.09
$(CO_2)_2$	146.14	-	262.38	320.5	378.62	436.74	494.86	-	611.1
$(CO_2)_3$	-	-	306.39	364.51	422.63	480.75	538.87	-	655.11
$(CO_2)_4$	234.16	-	350.4	408.52	466.64	524.76	582.88	-	-
$(CO_2)_5$	-	-	394.41	452.53	510.65	568.77	626.89	685.01	-
$(CO_2)_6$	-	-	438.42	496.54	554.66	612.78	670.9	-	-
$(CO_2)_7$	-	-	482.43	540.55	-	656.79	-	-	-
$(CO_2)_8$	-	-	526.44	-	-	-	-	-	-
$(CO_2)_9$	-	-	-	-	-	-	-	-	-
$(CO_2)_{10}$	-	-	614.46	-	-	-	-	-	-

References

[1] Stefan Feusi, Felix Graber, Jai Khatri, Chenxi Li, and Ruth Signorell. How CO_2 gas accelerates water nucleation at low temperature. *Journal of Chemical Physics*, 161(18):184304, nov 2024.

[2] Peter Stephan, Stephan Kabelac, Matthias Kind, Dieter Mewes, Karlheinz Schaber, and Thomas Wetzel, editors. *VDI-Wärmeatlas: Fachlicher Träger VDI-Gesellschaft Verfahrenstechnik und Chemieingenieurwesen*. Springer Reference Technik. Springer Vieweg, Berlin, Heidelberg, 12 edition, 2019.